THE JOURNAL OF BIOLOGICAL CHEMISTRY VOL. 291, NO. 44, pp. 23036–23046, October 28, 2016

Palmitoylation of Progressive Rod-Cone Degeneration (PRCD) Regulates Protein Stability and Localization*

Received for publication, June 8, 2016, and in revised form, September 8, 2016 Published, JBC Papers in Press, September 9, 2016, DOI 10.1074/jbc.M116.742767

Joseph Murphy and Saravanan Kolandaivelu[1]

From the Department of Ophthalmology, West Virginia University Eye institute, Morgantown, West Virginia 26506

Progressive rod-cone degeneration (PRCD) is a photoreceptor outer segment (OS) disc-specific protein with unknown function that is associated with retinitis pigmentosa (RP). The most common mutation in PRCD linked with severe RP phenotype is substitution of the only cysteine to tyrosine (C2Y). In this study, we find that PRCD is post-translationally modified by a palmitoyl lipid group at the cysteine residue linked with RP. Disrupting PRCD palmitoylation either chemically or by genetically eliminating the modified cysteine dramatically affects the stability of PRCD. Furthermore, *in vivo* electroporation of PRCD C2Y mutant in the mouse retina demonstrates that the palmitoylation of PRCD is important for its proper localization in the photoreceptor OS. Mutant PRCD C2Y was found in the inner segment in contrast to normal localization of WT PRCD in the OS. Our results also suggest that zDHHC3, a palmitoyl acyltransferase (PAT), catalyzes the palmitoylation of PRCD in the Golgi compartment. In conclusion, we find that the palmitoylation of PRCD is crucial for its trafficking to the photoreceptor OS and mislocalization of this protein likely leads to RP-related phenotypes.

Retinitis pigmentosa (RP)[2] is an inherited retinal disorder characterized by the progressive loss of photoreceptor cells leading to blindness (1, 2). RP is the most common blinding disease worldwide with a prevalence of 1 in 4000 (3–6). To date, there have been over 50 genes including *PRCD* that are linked to RP (1, 7).

PRCD is a highly conserved small 53–54-amino acid residue-long protein (8, 9). So far, six mutations in PRCD are linked to RP in humans (8, 10–12). Among these mutations, the most common is homozygous C2Y observed in humans and 29 different dog breeds (8, 13). This sole cysteine in PRCD is highly conserved among vertebrate species (8, 12, 13). In dog, cysteine mutation leads to disorganization of photoreceptor outer segment disc membranes (14, 15). However, the precise role of PRCD in photoreceptor neurons is still unclear.

A proteomic study demonstrated that PRCD is one of 11 proteins exclusively present in the photoreceptor outer segment (OS) disc membrane (16). The presence of PRCD within the OS disc membranes suggests that it plays an important role in photoreceptor function and/or maintenance. However, unlike the other proteins present in the OS disc, PRCD has no known function. Furthermore, association with the disc membrane is perplexing because PRCD has no known transmembrane domain. However, it is likely that the predicted N-terminal α-helix contributes to the interaction of PRCD with membranes. Interestingly, multiple mutations in this highly conserved N-terminal region are associated with RP in humans, suggesting the importance of this region in PRCD function. Our sequence analysis predicts structural domains that include transmembrane helices (aa 3–15), a polybasic region (aa 16–18), and a unique cysteine in the N terminus at the second position (aa Cys-2), which is likely palmitoylated (predicted using the CSS-Palm site prediction software). Additionally, heterozygous mutations (R17C and R18*X*) in the polybasic region are linked with RP, indicating its importance in PRCD function (8, 11).

In this study, we investigate whether PRCD is modified by palmitoyl lipid and seek to understand its importance in retinal function. Multiple studies have shown a role for palmitoyl lipid modification in protein assembly, stability, and activity, as well as interactions with binding partners and membranes (17, 18). An interesting aspect of protein palmitoylation is its reversibility and therefore the ability to dynamically regulate the membrane association of proteins. Improper protein sorting associated with defective palmitoylation has been linked to a variety of diseases ranging from colorectal cancer, hepatocellular carcinoma, X-linked mental retardation, schizophrenia, and Huntington's diseases (18–20). In retina, palmitoylation of rhodopsin, the G protein-coupled receptor (GPCR) at cysteine residues 322 and 323, is crucial for its stability and proper function of rod photoreceptor cells (21, 22). The loss of palmitoylation in rhodopsin enhances the light-induced photoreceptor degeneration (21). In this study, we demonstrate that the palmitoylation of PRCD is crucial for protein stability and trafficking to subcellular compartments.

Results

PRCD, a Photoreceptor Outer Segment Disc-resident Protein, Is Post-translationally Modified by Palmitoylation—We used acyl resin-assisted capture (acyl-RAC) to isolate palmitoylated

* This work was supported by West Virginia University (WVU) startup funds (to S. K.) and WVU internal Research Funding Development Grant (RFDG) 10018012.2.NT10076W (to S. K.). The authors declare that they have no conflicts of interest with the contents of this article.

[1] To whom correspondence should be addressed: Dept. of Ophthalmology, West Virginia University Eye institute, One Medical Center Dr., Morgantown, WV 26506. Tel.: 304-598-5484; Fax: 304-598-6928; E-mail: kolandaivelus@wvuhealthcare.com.

[2] The abbreviations used are: RP, retinitis pigmentosa; PRCD, progressive rod-cone degeneration; hPRCD, human PRCD; HAM, hydroxylamine; OS, outer segment(s); IS, inner segment(s); acyl-RAC, acyl resin-assisted capture; CNGA, cyclic nucleotide-gated channel; 17-ODYA, 17-octadecynoic acid; 2-BP, 2-bromo palmitate; CAG, chicken β-actin promoter; PAT, palmitoyl acyltransferase; hRPE1, human retinal pigment epithelial cells 1; IRES, internal ribosome entry site; OCT, optimum cutting temperature; aa, amino acids; PBR, polybasic regions; P, postnatal day.

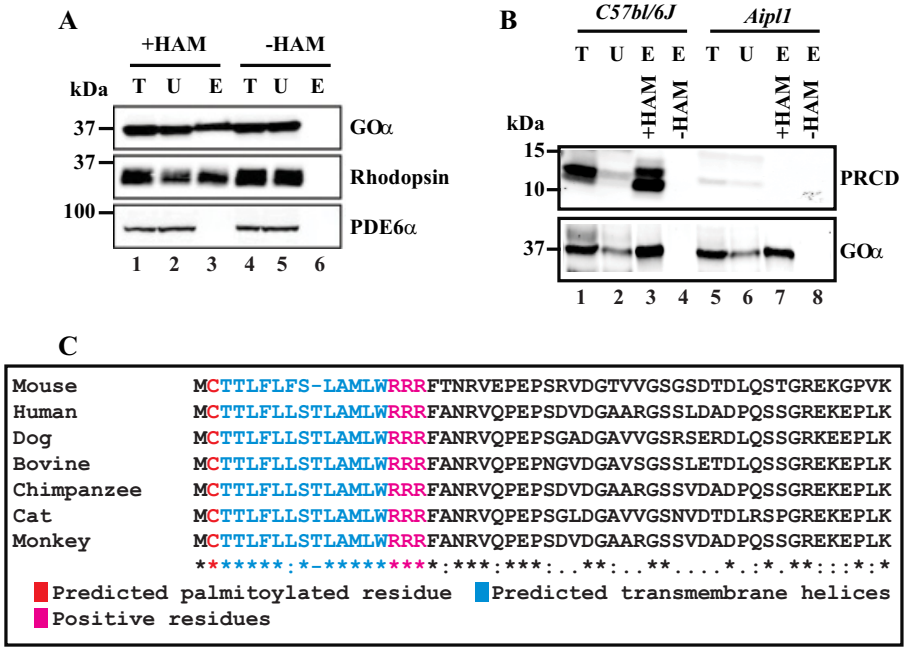

FIGURE 1. **PRCD is palmitoylated.** *A*, palmitoylated proteins from retinal extracts (P30, C57Black6/J) were enriched using the acyl-RAC method. Enriched proteins were then captured by thiopropyl-Sepharose column. Total (*T*) retinal extract, unbound (*U*) protein, and eluted protein (*E*) fractions from the column were separated by SDS-PAGE followed by immunoblotting with the indicated antibodies. $G_o\alpha$ and rhodopsin, known palmitoylated proteins, served as positive controls and were found only in +HAM-treated extracts (compare *lanes 3* and *6*). PDE6α, a non-palmitoylated protein, is a negative control. +HAM indicates treatment with hydroxylamine, whereas −HAM extracts were treated with vehicle control NaCl ($n = 6$). *B*, immunoblot identifying PRCD as a palmitoylated protein (*lane 3*, +HAM). PRCD protein is absent in the control (*lane 4*, −HAM). Retinal extracts from aryl hydrocarbon receptor-interacting protein like-1 (*Aipl1*) knock-out lack PRCD as indicated (*panel 1*, *lanes 5–8*). As a positive control, known palmitoylated protein $G_o\alpha$ is shown (*panel 2*, *lanes 3* and *7*, +HAM). *C*, a conserved cysteine residue (*red*), transmembrane helices (*blue*), and positively charged residues (*pink*) are indicated among vertebrate animals ($n = 6$).

proteins in mouse retina as described earlier (23, 24). Briefly, this method uses hydroxylamine to remove the labile palmitoyl group, leading to the generation of free cysteine residues in palmitoylated proteins. These proteins were then captured using a thiopropyl-Sepharose column. Retinal extracts were subjected to treatment with hydroxylamine (+HAM), and a portion of the extracts was treated with the vehicle NaCl (−HAM), which served as a control. To evaluate the validity of the method used, we first tested the enrichment of known palmitoylated proteins. Immunoblot of purified palmitoyl extract (+HAM) shows that the acyl-RAC method purifies $G_o\alpha$ and rhodopsin, in comparison with −HAM control (Fig. 1*A*) (25, 26). Phosphodiesterase-6 (PDE6) α subunit, a protein that is not palmitoylated, was not detected in the +HAM palmitoyl protein pool (Fig. 1*A*). These results demonstrate the robustness of the acyl-RAC assay in identifying palmitoylated proteins ($n = 6$). We then used this method to examine the palmitoylation of PRCD. Hydroxylamine cleavage and further capture by a thiopropyl-Sepharose column isolated a majority of PRCD present in retinal extracts from wild type animals (Fig. 1*B*, *lane 3*). In contrast, PRCD was not present in retina lacking photoreceptors (AIPL1-KO) (27) and consequently was not purified by the acyl-RAC method (Fig. 1*B*, *lane 7*). As a positive control, a known palmitoylated $G_o\alpha$ was purified from wild type and AIPL1-KO retinal extracts (Fig. 1*B*, *bottom panel*, *lanes 3* and *7*). Altogether, these results demonstrate that PRCD is potentially palmitoylated and is exclusively present in photoreceptor neurons.

C2Y Mutation Destabilizes PRCD—To evaluate the importance of palmitoylation in PRCD, we cloned gBlocks gene fragments of human wild type *PRCD* (*PRCD* WT) and mutants p.C2Y and p.V30M (*PRCD* C2Y and *PRCD* V30M, respectively) under the control of the ubiquitous chicken β-actin promoter (CAG) (Table 1) (28). Because PRCD is a small protein, we used a C-terminal HA tag to assess the PRCD protein stability. In the same construct, we used GFP as an internal control, which is independently driven by an internal ribosome entry site (IRES) (Fig. 2, *A* and *B*). The PRCD WT and mutant plasmids were transiently transfected into human retinal pigment epithelial cells 1 (hRPE1) cells. Immunoblotting analysis revealed a robust expression of PRCD WT in hRPE1 cells (Fig. 2, *C* and *D*). In contrast, expression of HA-tagged mutant PRCD C2Y was reduced by >90% (Fig. 2, *C* and *D*). The internal GFP, serving as a transfection control, showed similar expression in both PRCD WT-transfected and C2Y-transfected cells (Fig. 2*C*). To study the role of tyrosine in protein stability, we mutated cysteine to serine (p.C2S) instead of tyrosine. The C2S mutation exhibits similar results as C2Y, suggesting that the cysteine is playing a role in protein stability (Fig. 2*E*). These results imply that neither tyrosine nor serine affects the protein stability. To test whether destabilization of the protein is a common mechanism behind PRCD-RP, we examined the stability of another mutant V30M, which is also linked with human RP (8). In this case, unlike C2Y, the stability of the V30M mutant protein was similar to wild type PRCD (Fig. 2*F*).

Palmitoylation is the modification of cysteine residues with 16-carbon fatty acid palmitate. As indicated in Fig. 2*A*, the only cysteine residue in PRCD is in position 2, which is mutated to tyrosine (C2Y) in humans and multiple dog breeds (8, 9, 29). This change is expected to alter or inhibit the palmitoyl modi-

TABLE 1

The gBlocks fragments of human *PRCD* wild type and mutant gene sequences were synthesized from Integrated DNA Technologies used for cloning into pGAG-EGFP vector for cell culture and subretinal injection studies

The restriction sites for cloning in to pGAG-EGFP vector are underlined, and the bolded sequences in the 3′ sites represent the HA epitope tag. The changes made in the sequence according to human mutations are underlined and bolded.

PRCD gene gBlock fragment	Length (bases)	Sequence 5′ to 3′
HA-*hPRCD*-WT	234	ctgcgatcggtcgacccggtcgccaccatgtgcaccacccttttcctgctcagcaccctggccatgctctggcg ccgccgatttgccaaccgagtccaaccagagcccagcgacgtggatggggcagctaggggcagcagcttggat gcggaccctcagtcctcaggcagggagaaagaacctctgaag**tacccatacgatgttccagattacgct**taag gatccgagcgccgg
HA-*hPRCD*-C2Y	234	ctgcgatcggtcgacccggtcgccaccatgt**a**caccacccttttcctgctcagcaccctggccatgctctggcgc cgccgatttgccaaccgagtccaaccagagcccagcgacgtggatggggcagctaggggcagcagcttggatgc ggaccctcagtcctcaggcagggagaaagaacctctgaag**tacccatacgatgttccagattacgct**taaggat ccgagcgccgg
HA-*hPRCD*-V30M	234	ctgcgatcggtcgacccggtcgccaccatgtgcaccacccttttcctgctcagcaccctggccatgctctggcgcc gccgatttgccaaccgagtccaaccagagcccagcgac**a**tggatggggcagctaggggcagcagcttggatgcg gaccctcagtcctcaggcagggagaaagaacctctgaag**tacccatacgatgttccagattacgct**taaggatc cgagcgccgg

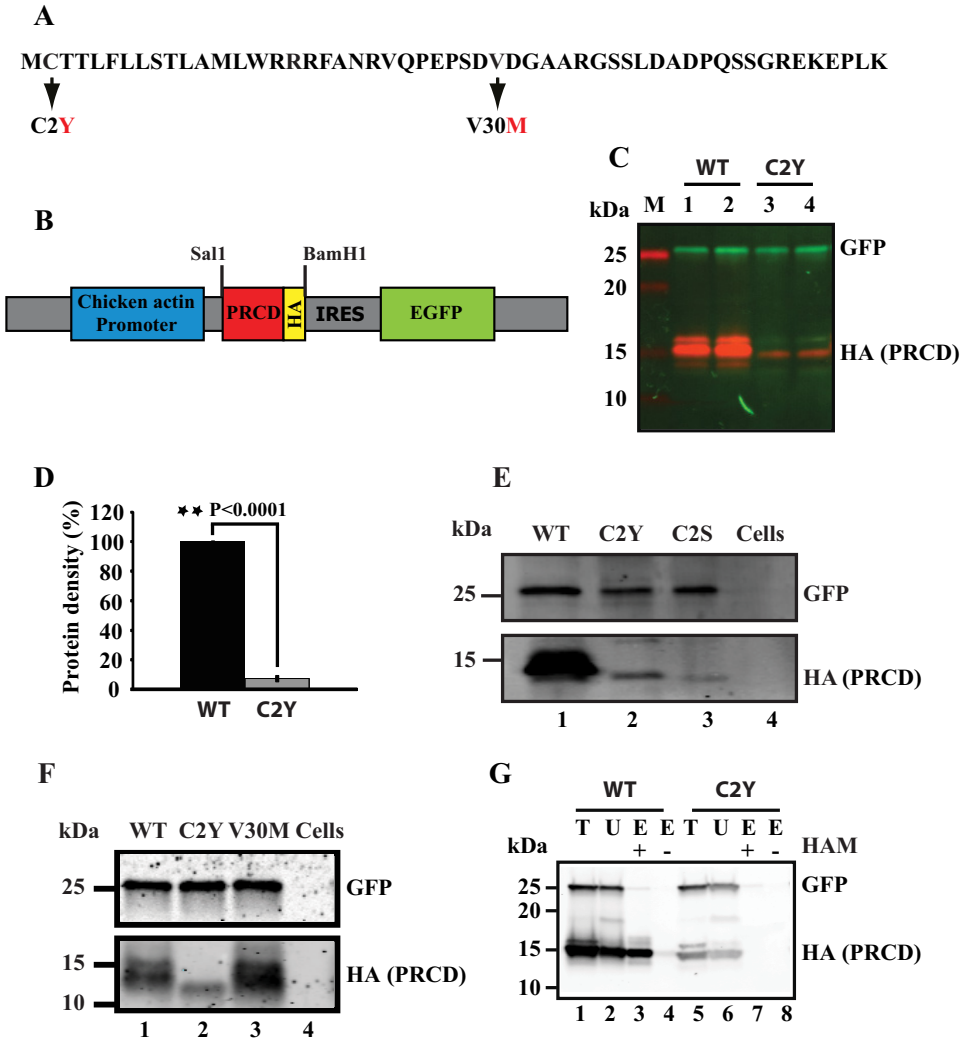

FIGURE 2. **Common mutation C2Y in PRCD leads to protein instability.** *A*, amino acid sequence of the entire PRCD protein with patient mutations indicated in *red*. *B*, scheme showing the cloning cassette used for exogenous expression of wild type PRCD and mutants. *C*, expression of transiently expressed PRCD in hRPE1 cells assessed by immunoblotting with the indicated antibodies. *Lanes 1* and *2* represent duplicate samples from wild type PRCD-transfected cell extracts, while *lanes 3* and *4* are from C2Y mutant-transfected cell extracts. Uniform GFP expression shown at the top served as an internal control ($n = 3$). *D*, quantitation of PRCD expression from *panel C*. PRCD expression was normalized to the internal GFP controls (**, $p < 0.0001$; $n = 3$). *E*, immunoblot shows that the cysteine residue in PRCD is important for PRCD stability (*lane 1*). Mutating cysteine to tyrosine or serine does not alter the protein stability (*lanes 2* and *3*). The hRPE1 cells served as a control and did not express PRCD protein ($n = 3$). *F*, similar to wild type, PRCD V30M mutation did not affect protein stability. GFP served as an internal control ($n = 3$). *G*, transiently expressed PRCD in hRPE1 is palmitoylated (*lane 3*, +HAM). The experimental strategy used for assaying palmitoylation is as described in Fig. 1. The C2Y mutant PRCD is not palmitoylated (*lane 7*). Non-palmitoylated GFP served as an internal control ($n = 3$). *T*, total retinal extract; *U*, unbound protein; *E*, eluted protein.

fication. To test this, we first evaluated the palmitoylation of PRCD WT using the acyl-RAC method as described earlier. Our results show that the PRCD WT transiently expressed into hRPE1 cells is palmitoylated (Fig. 2*G*, *lane 3*). In contrast, C2Y mutant, although reduced in expression, was not palmitoylated as judged by acyl-RAC method (Fig. 2*G*, *lane 7*). Collectively, these results suggest that palmitoylation in the PRCD protein is essential for the stability of PRCD.

Palmitoylation of PRCD Is Needed for Protein Stability—Protein instability in PRCD C2Y mutant could be due to defective protein palmitoylation or to the loss of the cysteine. To differentiate these possibilities, we inhibited palmitoylation using the non-metabolizable palmitate analog 2-bromopalmitate (2-BP), a widely used palmitoyl inhibitor (30–32). Human RPE1 cells transiently transfected with PRCD WT, PRCD C2Y, and PRCD V30M were treated with 150 μM 2-BP and vehicle DMSO for 24 h after transfection. The palmitoylation of PRCD WT treated with 2-BP was reduced by about 75% when compared with vehicle DMSO, whereas no change was observed in PRCD C2Y protein treated with 2-BP and vehicle DMSO (Fig. 3, *A* and

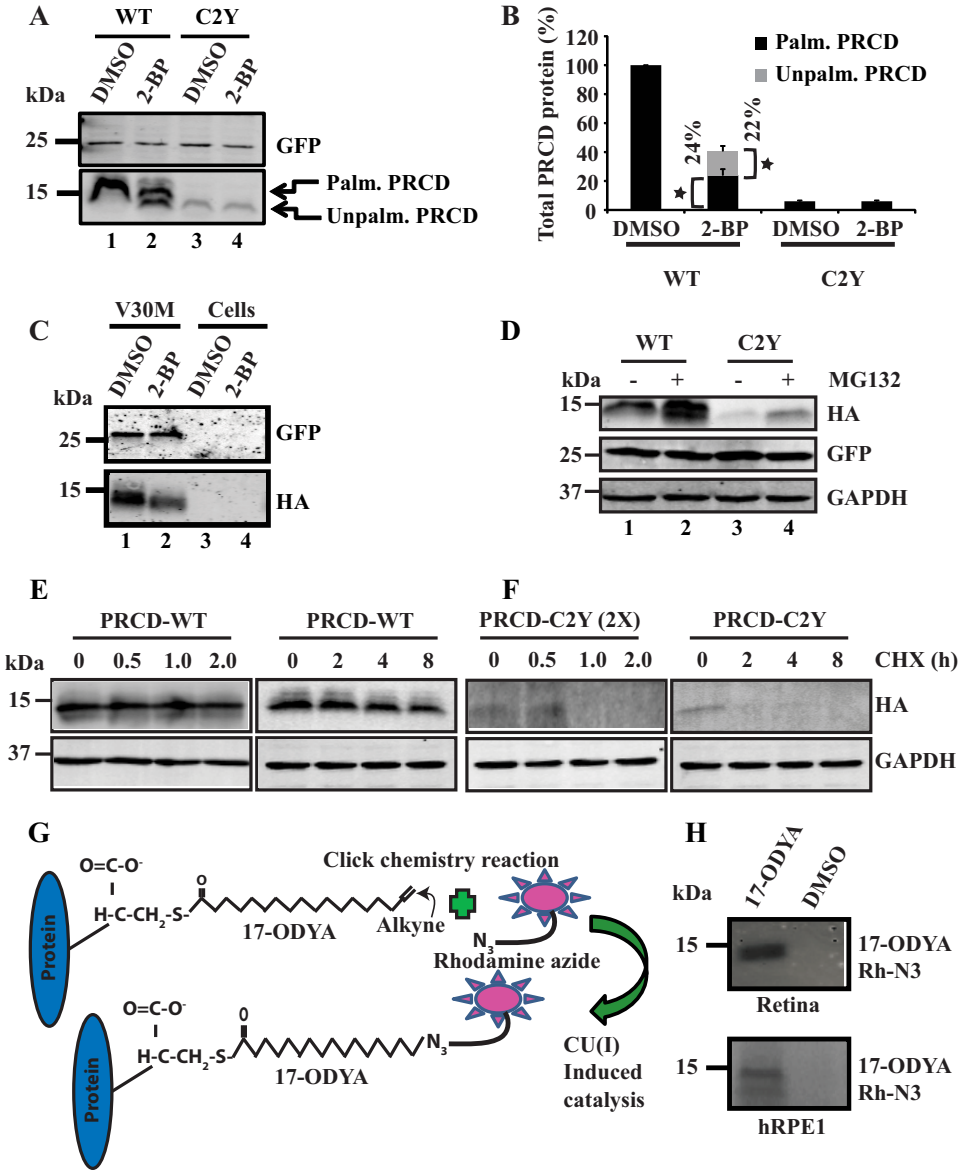

FIGURE 3. **Palmitoylation in PRCD is essential for its stability.** *A*, immunoblot shows the stability of wild type and C2Y mutant PRCD protein transiently expressed in hRPE1 cells after treatment with 2-BP (*bottom panel*, *lane 2*) and control treated with vehicle DMSO (*bottom panel*, *lane 1*). *Lanes 3* and *4* are mutant C2Y treated with vehicle DMSO and 2-BP. GFP was used as an internal control (*top panel*) ($n = 4$). Palm., palmitoylated; *Unpalm*, unpalmitoylated. *B*, graph represents the percentage of the density of palmitoylated *versus* unpalmitoylated PRCD protein after treating with 2-BP and vehicle DMSO (*, $p < 0.005$; $n = 4$). *C*, immunoblot shows that inhibition of palmitoylation by 2-BP destabilizes the V30M mutant PRCD transiently transfected in hRPE1 cells. GFP and untransfected hRPE1 cells served as a control ($n = 3$). *D*, Western blotting analysis of wild type and mutant (C2Y) PRCD treated with 20 μM MG132 or with vehicle for 8 h. GFP and GAPDH served as internal and loading controls ($n = 3$). *E* and *F*, Western blotting analysis of hRPE1 cells expressing PRCD wild type and C2Y mutant treated with 50 μg/ml cycloheximide (*CHX*) for 0, 0.5, 1.0, and 2 h (*first panel*. The *second panel* shows a longer incubation time with cycloheximide (0, 2, 4, and 8 h). GAPDH was used as a loading control ($n = 3$). *G*, a schematic illustration showing the metabolic labeling of PRCD with 17-ODYA, a palmitoyl chemical analog. *H*, retinal *ex vivo* culture of P10 retina used for metabolic labeling with 17-ODYA. The 17-ODYA incorporation was detected by the click chemistry method by copper-catalyzed TAMRA azide incorporation using copper (CU-1)-induced catalysis and detected by a Typhoon fluorescence scanner. Vehicle control (DMSO) shows no detection. Similarly, 17-ODYA incorporation was detected in wild type PRCD transiently expressed in hRPE1 cells (*bottom panel*, *lane 1*). Vehicle control (DMSO) experiments performed along with 17-ODYA are indicated with no detection (*top* and *bottom panel*, *lane 2*) ($n = 3$). *Rh-N3*, rhodamine azide.

B). Similar to PRCD WT, PRCD V30M mutant protein levels were reduced by 65% after treatment with 2-BP (Fig. 3*C*). As expected, no changes have been observed in GFP protein levels in the cells treated with 2-BP (Fig. 3, *A* and *C*). Taken together, these results demonstrate that palmitoylation is crucial for the stability of PRCD protein.

Furthermore, to analyze destabilization of PRCD C2Y mutant protein, we treated cells with the proteasome inhibitor MG132 (10 μM) (33, 34). We observed that the stability of mutant (C2Y) PRCD was elevated by 3-fold when compared with vehicle DMSO-treated cells (Fig. 3*D*, *compare lanes 3 and 4*). Also, the levels of wild type PRCD in cells treated with MG132 increased by 2-fold when compared with vehicle DMSO control (Fig. 3*D*, compare *lanes 1* and *2*). These results suggest that palmitoylation is necessary for protein stability, and palmitoylation-deficient PRCD undergoes rapid proteolytic degradation. To understand further, we have compared the decay of both wild type and mutant (C2Y) PRCD in hRPE1 cells treated with cycloheximide, a protein synthesis inhibitor that blocks *de novo* protein synthesis (35). We found that C2Y mutant protein levels were significantly destabilized within an hour when compared with wild type PRCD (Fig. 3, *E* and *F*). The levels of control GAPDH did not show any changes (Fig. 3, *E* and *F*). In sum, these results demonstrate that palmitoylation in PRCD is important for protein stability. In the absence of palmitoylation, PRCD undergoes rapid proteasome degradation within an hour of its synthesis.

As an independent approach to confirm the palmitoylation of PRCD, we cultured retina from C57Black6/J animals in the presence of alkyne fatty acid analog 17-octadecynoic acid (17-ODYA). Previous studies have shown that 17-ODYA is incorporated into endogenous palmitoylation sites (30, 31). We performed *ex vivo* PRCD palmitoylation in murine retina treated with 20 μM 17-ODYA or with vehicle control DMSO. These retinas were used for immunoprecipitation with affinity-purified PRCD antibody. To visualize 17-ODYA incorporation, we performed "click chemistry" with tetramethylrhodamine (TAMRA) azide by a copper-catalyzed reaction (31) (Fig. 3*G*). Click chemistry identified PRCD exclusively in retina incubated with 17-ODYA when compared with vehicle DMSO (Fig. 3*H*, *top panel*). A similar experiment testing 17-ODYA incorporation was performed with hRPE1 cells transiently transfected with HA-tagged human PRCD WT (Fig. 3*H*, *bottom panel*). Similar to the retinal *ex vivo* experiment, we observed incorporation of the palmitoyl analog in PRCD WT when compared with vehicle DMSO-treated cells (Fig. 3*H*, *bottom panel*). In contrast, we did not observe any detectable incorporation of 17-ODYA in cells expressing mutant C2Y in agreement with our earlier results showing that this PRCD mutant is defective for palmitoyl modification (data not shown). Overall, these results confirm PRCD palmitoylation in native retinal tissue and cell culture, and show that palmitoylation in PRCD is crucial for protein stability.

Palmitoylation Is Important for Proper Targeting and Localization—We examined the localization of PRCD in the mouse retina using our custom-generated PRCD antibody and found that PRCD is localized in the photoreceptor OS. Cyclic nucleotide-gated channel (CNGA1/3), a known marker for photoreceptor OS, was used as a control. Our results show exclusive localization of PRCD in the photoreceptor OS in agreement with previously published results (Fig. 4*A*) (16). However, the mechanism of exclusive targeting and localization of PRCD in the photoreceptor OS is unclear. To understand the importance of palmitoylation in PRCD protein trafficking, we introduced plasmids expressing HA-tagged PRCD WT and C2Y into murine photoreceptor cells by subretinal injection followed by *in vivo* electroporation (Fig. 4*B*). Retinal sections show expression of PRCD WT in the photoreceptor OS (Fig. 4*B*, *top panel*), whereas GFP expression was mainly observed in the IS as observed in earlier studies (36, 37). In contrast, the mutant PRCD C2Y was co-localized with GFP in the IS (Fig. 4*B*, *lower panel*). We summarize based on these results that palmitoylation in PRCD is needed for targeting to the photoreceptor OS.

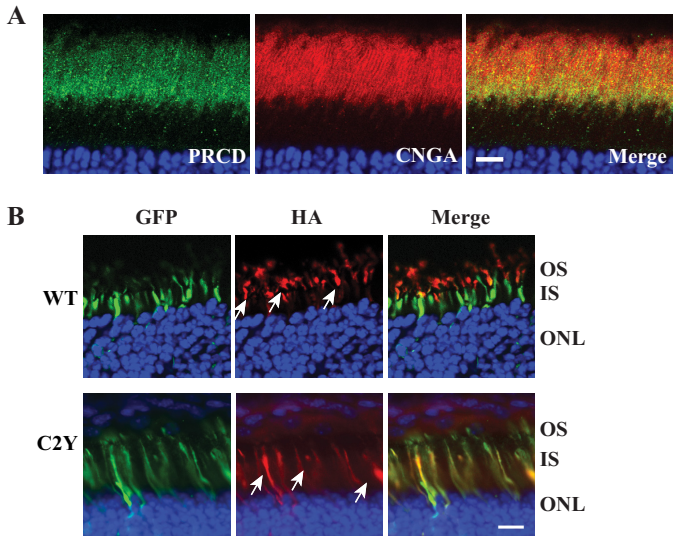

FIGURE 4. **Palmitoylation in PRCD is important for proper targeting and localization.** *A*, immunofluorescence of wild type (P30) frozen retinal section probed with anti PRCD and CNGA. PRCD is localized in the photoreceptor OS ($n = 3$). *B*, subretinal injection followed by *in vivo* electroporation of HA-tagged PRCD wild type in mouse retina localized in the photoreceptor OS. In contrast, mutant C2Y PRCD is mislocalized in the photoreceptor IS. GFP served as a transfection control ($n = 6$). *ONL*, outer nuclear layer.

Association of PRCD with Membranes Is Not Dependent on Palmitoylation—A previous study revealed that PRCD is one of 11 proteins exclusively present in the photoreceptor disc membrane (16). We wanted to investigate the contribution of protein palmitoylation in the membrane association of PRCD. We first determined the subcellular location of PRCD in transiently transfected hRPE1 cells. Our subcellular fractionation showed that the majority (85%) of PRCD was present in the membrane fraction (Fig. 5*A*). Interestingly, wild type PRCD treated with palmitoyl inhibitor (2-BP) and severely destabilized PRCD C2Y mutant were also enriched in the membrane fraction (Fig. 5*A*). A marker for endoplasmic reticulum (calnexin) was used as a marker for membranes, and GAPDH was used as a cytosolic marker in the subcellular fractions. As a control, tubulin was observed in both soluble and membrane fractions (Fig. 5*A*). Overall, these results demonstrate that despite the loss of palmitoylation, exogenously expressed PRCD remains in the membrane fraction. To understand the need of palmitoylation

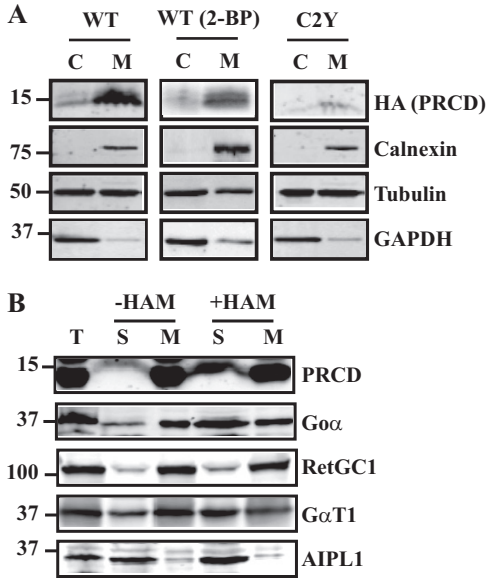

FIGURE 5. **Association of PRCD with membranes is not dependent on palmitoylation.** *A*, immunoblots of subcellular fractionated membranes from hRPE1 cells transiently transfected with wild type, wild type treated with palmitoyl inhibitor 2-BP, and mutant PRCD C2Y show a majority of PRCD remains in the membrane fraction (*M*) despite the lack of palmitoylation. Calnexin (endoplasmic reticulum marker), tubulin, and GAPDH served as controls ($n = 3$). *C*, cytoplasmic fraction; *M*, membrane fraction. *B*, membrane fractionation from mouse retinal lysate treated with 300 μM HAM shows that ~80% of PRCD remains in the membrane fraction when compared with control (−HAM). The distributions of $G_o\alpha$, a known palmitoylated protein, membrane-bound RetGC1, $G\alpha_{T1}$, and cytosolic AIPL1 are indicated ($n = 3$). *T*, total; *S*, soluble; *M*, membrane.

in PRCD for its membrane association, we examined PRCD membrane association in native retinal lysates after removal of the palmitoyl group by HAM. Our results show that the majority of PRCD remains in the membrane fraction even after treatment with 300 μM HAM. In contrast, $G_o\alpha$, a known palmitoylated protein dependent on the palmitoyl group for membrane attachment, was found in the soluble fraction after HAM treatment (Fig. 5*B*). As controls, the transmembrane protein retinal guanylate cyclase (RetGC1) and rod transducin α subunit did not exhibit any change in distribution after HAM treatment (Fig. 5*B*). As a cytosolic marker, we used AIPL1, which is present in the soluble fraction, and no changes were observed after HAM treatment (Fig. 5*B*). Together with these results, we speculate that the palmitoylation of PRCD is not the major determinant for its membrane association.

Palmitoylation Enzyme zDHHC3 Augments PRCD Palmitoylation and Stability—Palmitoylation is catalyzed by the zDHHC (Asp-His-His-Cys zinc finger) family of palmitoyl acyltransferase (PAT) proteins typically located in endomembranes (38). To identify the PAT that influences the palmitoylation and stability of PRCD, we screened several PAT enzymes by co-transfecting with PRCD constructs in hRPE1 cells. The screened PAT enzymes were selected based on their expression pattern within the retina (39). Among zDHHCs 2, 3, 5, and 6 that were co-transfected with PRCD (Fig. 6*D*), the most striking difference in the levels of PRCD and its palmitoylation was observed with zDHHC3 (Fig. 6, *A*–*C*). In comparison, zDHHCs 2, 5, and 6 did not show appreciable enhancement of PRCD levels, suggesting that zDHHC3, a Golgi-resident PAT enzyme, is likely responsible for PRCD palmitoylation (Fig. 6) (32, 41). As expected, no obvious differences were observed in PRCD C2Y mutant (Fig. 6*A*). As described earlier, GFP was used as an internal control for protein stability (Fig. 6*A*, *top panel*). Furthermore, the palmitoylation status of PRCD protein co-expressed with zDHHC3 is enhanced approximately 5-fold higher than the control that lacks DHHC3 overexpression (Fig. 6*C*, *+HAM*). These results suggest that PRCD is palmitoylated by zDHHC3 at the Golgi compartments. Defects in this process lead to mistargeting of the PRCD protein, followed by severe reduction in protein level by proteolytic degradation.

Discussion

The present study demonstrates that the sole cysteine residue in PRCD associated with RP in humans and multiple dog breeds (C2Y) is post-translationally lipid-modified by palmitoylation. Furthermore, palmitoylation is essential for protein stability and targeting to photoreceptor outer segments. Our studies also show that PRCD is strongly associated with the membrane and that this association is independent of its palmitoylation status.

Protein palmitoylation is a common post-translational lipid modification in a protein, where a 16-carbon palmitic acid is attached to the cysteine residue through a reversible thioester linkage. Unlike prenylation and myristoylation, palmitoylation is unique in that it is a reversible process and there is no consensus sequence requirement. Protein palmitoylation contributes to various cell signaling events including membrane association, protein trafficking, and stability (18, 42). Defects in palmitoylation are also implicated in a variety of diseases (20, 42). In retina, abolishing palmitoylation in rhodopsin leads to visual impairment and light-induced photoreceptor degeneration (21). However, the importance of palmitoylation and the palmitoylated substrates in retinal photoreceptor neurons is poorly understood. The present study confirms PRCD palmitoylation by multiple approaches in both native retinal tissues and an *in vitro* cell culture systems, and shows that defective palmitoylation profoundly affects the stability of the PRCD protein.

Although it is clear that palmitoylation affects the post-translational stability of PRCD, lipid modification does not play a significant role in membrane association. Because PRCD does not have a known transmembrane domain, the strong membrane association is unclear. We speculate that the highly conserved N-terminal region of PRCD that is predicted as transmembrane helices (aa 3–15) could be a primary determinant for PRCD peripheral membrane association. In addition to this, we also believe that a potential polybasic region (aa 16–18) adjacent to transmembrane helices plays a synergistic role in membrane attachment. Polybasic regions (PBR) in small GTPases such as K-Ras4B have been shown to enhance membrane association with negatively charged phospholipids in the plasma membrane (43, 44). We speculate that the PBR in PRCD could be contributing similarly along with adjacent hydrophobic transmembrane helices. Interestingly, there are two mutations in the PBR of PRCD (R18*X*, R17C) that are associated with blinding diseases. The R17C mutation in particular might indicate the importance of PBR that could be further evaluated for

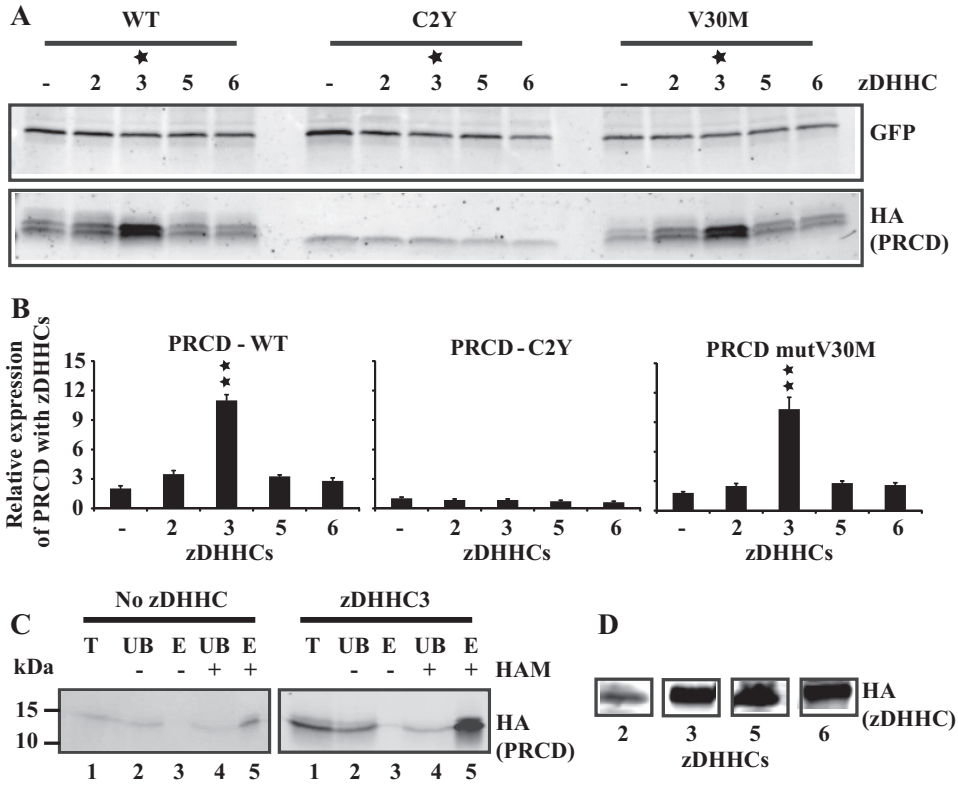

FIGURE 6. **PAT zDHHC3 enhances PRCD palmitoylation and stability.** *A*, selected zDHHC plasmids were transiently co-transfected with wild type and PRCD mutant plasmids (C2Y and V30M) into hRPE1 cells. The immunoblotting analysis shows that the zDHHC3 enzyme enhances wild type PRCD by 5-fold higher when compared with control (*lane 1*), while other enzymes (DHHCs 2, 5 and 6) did not show any significant enhancement of PRCD. C2Y mutant PRCD did not show any changes in protein levels when co-transfected with zDHHCs. The stability of PRCD mutant V30M was enhanced similar to the wild type. GFP served as an internal control ($n = 3$). *B*, graph shows the relative expression of wild type and C2Y mutant PRCD protein (C2Y and V30M) with zDHHCs (**, $p < 0.0001$; $n = 3$). *C*, immunoblots of palmitoyl assay samples purified by the acyl-RAC method show robust expression and the palmitoylation of wild type PRCD with zDHHC3 when compared with control with no zDHHC3 (*lanes 1* and *5*). No proteins were observed in −HAM samples (*lane 3*) ($n = 3$). *T* = total, *UB* = unbound, *E* = elution. *D*, immunoblots of zDHHCs protein levels transiently transfected in hRPE1 cells ($n = 3$).

understanding the specific role of PBR in PRCD membrane association (8, 11).

Although it is clear that factors other than palmitoylation are contributing to membrane association, our studies indicate that palmitoylation is crucial for proper OS localization. Our *in vivo* electroporation studies show a clear discrepancy in localization of palmitoylation-deficient PRCD. Our results strongly support the idea that post-translational lipid modification is required for PRCD to properly associate with the transport vesicles and ultimately traffic to the OS. The loss of palmitoylation could result in aggregation of protein in the cytoplasm/endomembrane, leading to severe proteolytic degradation.

The addition of palmitoyl lipid is catalyzed by PAT enzymes characterized by the presence of zDHHC domain in the endomembrane. We observed significant enhancement of PRCD palmitoylation in presence of zDHHC3, an enzyme that is present in the Golgi compartment (40, 41). It is important to note that the observed enhancement was specific and was not found when other zDHHCs were overexpressed. These results imply that PRCD palmitoylation is processed in the Golgi compartment. After synthesis in the cytosol, many peripheral membrane proteins are targeted to the Golgi for palmitoylation and then trafficked to their destination (45). Overall, our findings suggest that the palmitoylation process in PRCD is crucial for efficient trafficking to the photoreceptor OS. We believe that lack of palmitoylation could cause two problems that proceed to cellular dysfunction: 1) defects in trafficking to photoreceptor OS, and 2) mistrafficking and aggregation in subcellular compartments. The latter of these may be creating additional cellular stress, which would cause protein destabilization and photoreceptor dysfunction.

In conclusion, this is the first study that reveals palmitoyl lipid modification in a photoreceptor disc-specific protein, PRCD, that is linked with RP blinding disease. Our findings show that palmitoylation is crucial for protein stability and is needed for trafficking of PRCD to photoreceptor OS. As demonstrated earlier in canine models, the C2Y mutation in PRCD leads to disorganization of photoreceptor OS disc membranes due to defects in renewal and/or phagocytosis (14, 15). However, the precise role of PRCD in photoreceptor function and OS maintenance needs to be clarified further.

Experimental Procedures

Animals—All handling, care, and experimental procedures involving animals were performed in accordance with the National Institutes of Health guidelines, and the protocol was approved by the Institutional Animal Care and Use Committee (IACUC) at West Virginia University.

Reagents and Antibodies—Cell cultures were maintained in DMEM/F12 containing L-glutamine and 15 mM HEPES (Medi-

atech Inc. Manassas, VA). FBS and antibiotics (penicillin-streptomycin solution) were obtained from HyClone Laboratories, Logan, UT. Trypsin (0.25%) EDTA (1 mM) was obtained from GIBCO, Life Technologies. MG132 was obtained from Cayman Chemical Co. (Ann Arbor, MI), and cycloheximide was from Calbiochem. The PRCD antiserum was raised in rabbits using a peptide antigen (C-terminal peptide, CDGTVVGSGSDTDLQSTGREKGPVK) that corresponds to the mouse PRCD by Pacific Immunology, Ramona, CA. The antibody was affinity-purified using the antigen peptide coupled to sulfo-link resin (Thermo Scientific). We also used the following commercial antibodies and reagents: anti-GFP (Millipore); HA (Sigma-Aldrich); CNGA-1/3 (NeuroMab); calnexin (Novus); tubulin (Sigma); RetGC1 (Millipore); PDE6α (Millipore); Gα_{T1} and G$_o\alpha$ (Santa Cruz Biotechnology); and GAPDH mouse monoclonal antibody 10RG109a (Fitzgerald Industries).

Acyl-RAC Purification of Palmitoylated Proteins—Palmitoyl modification of PRCD was assessed using previously published methods (23, 24). Retina or transiently transfected hRPE1 cells were homogenized in ice-cold lysis buffer (25 mM HEPES, pH 7.5, 150 mM NaCl, 1 mM EDTA, 0.5% Triton X-100 plus protease and phosphatase inhibitors). After a brief centrifugation at 500 × *g* for 5 min, the supernatant was collected into another tube and the free cysteine residues present in supernatant (~2 mg of total protein) were blocked with *S*-methyl methanethiosulfonate (Sigma) in the blocking buffer (100 mM HEPES, pH 7.5, 1 mM EDTA, 0.1% *S*-methyl methanethiosulfonate plus 2.5% SDS) at 40 °C for 10 min. Proteins were precipitated with ice-cold acetone kept at −20 °C for 30 min and centrifuged at 10,000 × *g* for 12 min at 4 °C, and pellets were washed five times with 70% ice-cold acetone. After a thorough wash, the pellet was air-dried at room temperature for 10 min and re-suspended with 300 μl of binding buffer (100 mM HEPES, 1 mM EDTA, 1% SDS plus protease and phosphatase inhibitors). To this mixture (250 μl), 40 μl of thiopropyl-Sepharose beads (GE Healthcare) and 40 μl of 2 M hydroxylamine were added. For the control, 40 μl of 2 M NaCl was added to another tube containing samples with thiopropyl-Sepharose beads. After incubation for 3 h at room temperature, beads were washed four times with binding buffer, and the proteins were eluted from the column with binding buffer containing 50 mM DTT. The eluted proteins were further analyzed by SDS-PAGE electrophoresis and Western blotting. Membranes were scanned using an Odyssey Infrared Imaging System (LI-COR Biosciences).

Cloning and Cell Transfection—The human *PRCD* constructs encoding wild type and mutants (C2Y and V30M) with the C-terminal HA epitope-tagged gBlocks gene fragments (200 ng) were custom-synthesized from Integrated DNA Technologies. These epitope-tagged gene fragments were cloned into pCAG vector under CAG, and in-frame with IRES-EGFP, they were transiently expressed in the hRPE1. Table 1 presents details of gBlocks *PRCD* sequence constructs for both WT and mutants.

The hRPE1 were maintained in DMEM/F12 medium supplemented with 10% FBS and 1% penicillin and streptomycin in a sterile incubator at 37 °C and 5% CO_2. Cells were cultured in 100 × 20-mm dishes for 72 h. Confluent cells were disassociated with 1 ml of 0.25% trypsin-EDTA and seeded for transient transfections in 6-well plates at 4.5×10^4 cells/well. Cells were transfected 24 h after plating with transfection reagent TansLT1 (6 μl/well), serum-free medium (0.25 ml/well), and plasmid DNA at 2.4 μg/well. At 24 h after transfection, the cells were treated with 150 μM 2-BP, or at 48 h after transfection, treated with 20 μM MG132 (8 h), or to block the *de novo* protein synthesis with cycloheximide (50 μg/ml), treated with different timing (0, 0.5, 1, 2, 4, and 8 h). Cells were collected at 48 h after transfection with Hanks' balanced salt solution containing 1 mM EDTA and prepared for protein analysis as described below.

Metabolic Labeling—Palmitoyl chemical analog 17-ODYA (Cayman Chemical Co.) was used for metabolic labeling. Transient transfection of PRCD wild type and C2Y mutant with 70% confluence hRPE1 cells in 100-mm tissue culture dishes was performed with 100 μM 17-ODYA or vehicle DMSO for 48 h (30, 46). To facilitate dissolution of 17-ODYA in the medium, 75 μl of 20 mM 17-ODYA stock in DMSO (or vehicle DMSO only) was mixed with 150 μl of 10% fatty acid-free bovine serum albumin (Sigma) and was added to 15 ml of DMEM, and the mixture was vortexed prior to being added to cells. After 48 h, the cells were collected in 1.5-ml Eppendorf tubes and lysed with 1× PBS containing protease and phosphatase inhibitors, 10 μM HDSF and 1.0% Triton X-100, and detergent-soluble proteins pellets were collected by centrifugation (12,000 × *g* for 10 min). Mouse retinal PRCD was immunoprecipitated by affinity-purified polyclonal anti-PRCD (rabbit), and hRPE1 cells transiently expressing PRCD were immunoprecipitated by HA beads. The copper-catalyzed click chemistry reaction was performed in beads using azide-rhodamine as described by the manufacturer (Invitrogen). Samples were prepared in 1× Laemmli sample buffer containing 2-β-mercaptoethanol. Samples were not boiled prior to SDS-PAGE. Labeled proteins were separated by SDS-PAGE, and rhodamine azide-labeled proteins were detected by a Typhoon scanner (Bio-Rad).

Immunocytochemistry—Human RPE-1 cells were seeded onto coverslips in 6-well plates and transfected 24 h after plating with wild type or mutant PRCD constructs. After 48 h of growth, cells were washed with 1× PBS and fixed in 4% paraformaldehyde for 15 min. Fixed cells were washed with 1× PBS, permeabilized with cold methanol for 10 min, and washed three times with 1× PBS before blocking with 2% goat serum solution for 1 h. Blocked cells were incubated overnight in 1× PBS containing 0.1% Triton X-100 (PBS-Triton) and primary antibody overnight at 4 °C. Cells were washed with 1× PBS containing 0.1% Triton X-100 before incubation with secondary antibody and DAPI for 1 h. Cells were then washed with PBS-Triton X-100 and mounted with ProLong Gold mounting solution (Life Technologies).

Immunohistochemistry—Enucleated mouse eyes were punctured with a needle and fixed with 4% paraformaldehyde (Electron Microscopy Sciences, Hatfield, PA) at room temperature for 10 min. Eyecups were processed after removal of both cornea and lens, and the tissue was further fixed in 4% paraformaldehyde for 1 h at room temperature. Eyecups were cryoprotected in 20% sucrose in 1× PBS overnight at 4 °C. The tissue was then frozen in optimal cutting temperature compound (OCT) on dry ice and stored at −80 °C. Cryosections were cut

at 16 μm and collected on Superfrost Plus slides (Fisher Scientific). For immunohistochemistry, the OCT was washed three times with 1× PBS and incubated in block buffer containing 2% goat serum for 1 h prior to incubation with primary antibody overnight at 4 °C. Primary antibody was washed with 1× PBS containing 0.1% Triton X-100, and sections were incubated in the appropriate secondary antibody (Odyssey Alexa Fluor 488 or Alexa Fluor 568, LI-COR Biosciences, diluted with the same buffer used for the primary antibody) at 1:1,000 dilutions for 1 h at room temperature. DAPI (1:5000, Molecular Probes) used as a nuclear stain was added with secondary antibody. Slides were mounted with ProLong Gold antifade reagent (Life Technologies) and coverslipped (1 mm). Confocal imaging was performed at the WVU microscope imaging facility with a Zeiss LSM 510 laser scanning confocal on an LSM Axioimager upright microscope using excitation wavelengths of 405, 488, and 543 nm.

Retinal PRCD Extraction—Flash-frozen C57/black/129 SvE retinal tissues were homogenized four times with ice-cold isotonic buffer (1× PBS) containing protease and phosphatase inhibitors. The retinal lysates were centrifuged at 300 × *g* for 4 min to remove tissue debris. The supernatants were collected into two fresh tubes and labeled as +HAM (300 μM hydroxylamine) and −HAM (300 μM NaCl). Equal volumes of protein samples were incubated at room temperature for 2 h with + or −HAM. After incubation, samples were centrifuged at 45,000 rpm for 15 min at 4 °C. The soluble supernatant fraction was collected to a fresh Eppendorf tube, and the pellet fraction was re-suspended with an equal volume of isotonic buffer. Fractions obtained were prepared for Western blotting with the indicated antibodies as described in the "Immunoblotting" section.

Subcellular Protein Fractionation—For the subcellular protein fractionation study, we used a subcellular fractionation kit for cultured cells (Thermo Scientific). We performed experiments as per the manufacturer's instructions. Transiently transfected hRPE1 cells with HA-tagged WT and mutant (C2Y) PRCD were harvested at 48 h after transfection. The pelleted cells were re-suspended in cytoplasmic extraction buffer containing protease inhibitor, incubated at 4 °C for 10 min, and centrifuged at 500 × *g* for 5 min to obtain cytosolic fraction. The pellet was re-suspended with ice-cold membrane extraction buffer, vortexed, incubated at 4 °C for 10 min, and then centrifuged at 3000 × *g* for 5 min at 4 °C. The membrane extract supernatant fractions were collected to another tube. The resulting pellets were used for preparing soluble nuclear extract and chromatin-bound nuclear extract using NEB buffer (New England Biolabs) and NEB buffer containing $CaCl_2$ and micrococcal nuclease as per the manufacturer's instructions. Each fraction was analyzed for PRCD localization by Western blotting using anti-HA antibody. Immunoblotting and protein density measurements were performed as described in the "Immunoblotting" section.

Immunoblotting—Flash-frozen retinal samples (C57black and129SvE) and lysates of hRPE1 cells transiently transfected with PRCD-expressing construct were homogenized by sonication (Microson Ultrasonic cell disruptor) in 1× PBS containing protease and phosphatase inhibitors (Pierce). The protein concentration was measured by using a NanoDrop spectrophotometer (ND-1000, Thermo Scientific). Equal concentrations (150 μg) of total protein samples were resolved in 15% SDS-PAGE and then transferred to an Immobilon-FL membrane. Membranes were blocked with the Rockland blocking buffer for 60 min at room temperature. After blocking, membranes were incubated with primary anti-HA or anti-PRCD antibodies (1:2000), calnexin (Proteintech), tubulin (Sigma), $G_o\alpha$ (Santa Cruz Biotechnology), RetGC1, PDE6α (Thermo Fisher), and $G\alpha_{T1}$ (Santa Cruz Biotechnology) (at 1:2000 dilutions) for 2 h at room temperature. After washing the membrane four times with 1× PBST, the secondary antibodies, Odyssey goat anti-rabbit Alexa Fluor 680, Odyssey goat anti-rabbit Alexa 680, and goat anti-mouse 680 (LI-COR Biosciences) were used at a 1:50,000 dilutions for 30 min at room temperature. After washing three times with 1× PBST, membranes were scanned and protein density was measured using an Odyssey Infrared Imaging System (LI-COR Biosciences) according to manufacturer's instructions.

Subretinal Injection—Purified PRCD plasmid DNA at 2.5 μg/μl containing 0.1% fluorescein sodium (100 mg ml^{-1} AK-FLUOR, Alcon, Fort Worth, TX) was injected into the subretinal space of newborn CD-1 pups as described (40). After anesthesia, an incision was made at the future eyelid with a 33-gauge needle under a dissecting microscope. The needle was used to make a pinhole puncture in the sclera away from the lens. 0.5 μl of DNA was injected through the puncture into the subretinal space using a blunt-end syringe. Five pulses of 80 v at 50-ms duration with 950-ms intervals were then applied with tweezer-type electrodes, BTX model 520, 7-mm diameter. All experimental results and conclusions are based on at least three independent experiments

Immunoprecipitation—Cell pellets were re-suspended in 200 μl of 1× PBS containing protease inhibitors (Pierce) and homogenized by sonication (Microson Ultrasonic cell disruptor). Triton X-100 was added to a final concentration of 1% and incubated for 10 min prior to centrifugation. The supernatant was collected into a separate Eppendorf tube. 10 μl of HA (Roche Applied Science) and/or PRCD affinity matrix beads were added to each sample and incubated on a rotator at 4 °C for 3 h or overnight. After incubation, the samples were centrifuged, and a portion of the supernatant was collected. The beads were washed with 1× PBS containing 1% Triton X-100 before preparation for Western blotting analysis as described earlier.

Author Contributions—J. M. and S. K. performed experiments and analyzed data. S. K. conceived the idea of the project and the experimental design, and wrote the paper with J. M.

Acknowledgments—We thank Dr. Vadim Arshavsky for the generous gift of the PRCD antibody and Dr. Fukata for providing the zDHHCs clones. We also thank Drs. Ramamurthy, Sokolov, Mathers, and Stoilov and other lab members for their constant support.

References

1. Daiger, S. P., Bowne, S. J., and Sullivan, L. S. (2007) Perspective on genes and mutations causing retinitis pigmentosa. *Arch. Ophthalmol.* **125,** 151–158

2. Guadagni, V., Novelli, E., Piano, I., Gargini, C., and Strettoi, E. (2015) Pharmacological approaches to retinitis pigmentosa: a laboratory perspective. *Prog. Retin. Eye Res.* **48,** 62–81
3. Maubaret, C., and Hamel, C. (2005) [Genetics of retinitis pigmentosa: metabolic classification and phenotype/genotype correlations]. *J. Fr. Ophtalmol.* **28,** 71–92
4. Parmeggiani, F. (2011) Clinics, epidemiology and genetics of retinitis pigmentosa. *Curr. Genomics* **12,** 236–237
5. Hartong, D. T., Berson, E. L., and Dryja, T. P. (2006) Retinitis pigmentosa. *Lancet* **368,** 1795–1809
6. Kalloniatis, M., Nivison-Smith, L., Chua, J., Acosta, M. L., and Fletcher, E. L. (2015) Using the rd1 mouse to understand functional and anatomical retinal remodelling and treatment implications in retinitis pigmentosa: a review. *Exp Eye Res.* 10.1016/j.exer.2015.10.019
7. Fahim, A. T., Daiger, S. P., and Weleber, R. G. (2000) Retinitis pigmentosa overview. in *GeneReviews®* (Pagon, R. A., Adam, M. P., Ardinger, H. H., Wallace, S. E., Amemiya, A., Bean, L. J. H., Bird, T. D., Fong, C. T., Mefford, H. C., Smith, R. J. H., and Stephens, K. eds), pp. 1993–2015, University of Washington, Seattle, WA
8. Zangerl, B., Goldstein, O., Philp, A. R., Lindauer, S. J., Pearce-Kelling, S. E., Mullins, R. F., Graphodatsky, A. S., Ripoll, D., Felix, J. S., Stone, E. M., Acland, G. M., and Aguirre, G. D. (2006) Identical mutation in a novel retinal gene causes progressive rod-cone degeneration in dogs and retinitis pigmentosa in humans. *Genomics* **88,** 551–563
9. Goldstein, O., Zangerl, B., Pearce-Kelling, S., Sidjanin, D. J., Kijas, J. W., Felix, J., Acland, G. M., and Aguirre, G. D. (2006) Linkage disequilibrium mapping in domestic dog breeds narrows the progressive rod-cone degeneration interval and identifies ancestral disease-transmitting chromosome. *Genomics* **88,** 541–550
10. Nevet, M. J., Shalev, S. A., Zlotogora, J., Mazzawi, N., and Ben-Yosef, T. (2010) Identification of a prevalent founder mutation in an Israeli Muslim Arab village confirms the role of *PRCD* in the aetiology of retinitis pigmentosa in humans. *J. Med. Genet.* **47,** 533–537
11. Pach, J., Kohl, S., Gekeler, F., and Zobor, D. (2013) Identification of a novel mutation in the *PRCD* gene causing autosomal recessive retinitis pigmentosa in a Turkish family. *Mol. Vis.* **19,** 1350–1355
12. Remez, L., Zobor, D., Kohl, S., and Ben-Yosef, T. (2014) The progressive rod-cone degeneration (PRCD) protein is secreted through the conventional ER/Golgi-dependent pathway. *Exp. Eye Res.* **125,** 217–225
13. Kohyama, M., Tada, N., Mitsui, H., Tomioka, H., Tsutsui, T., Yabuki, A., Rahman, M. M., Kushida, K., Mizukami, K., and Yamato, O. (2016) Real-time PCR genotyping assay for canine progressive rod-cone degeneration and mutant allele frequency in Toy Poodles, Chihuahuas and Miniature Dachshunds in Japan. *J. Vet. Med Sci.* **78,** 481–484
14. Aguirre, G., Alligood, J., O'Brien, P., and Buyukmihci, N. (1982) Pathogenesis of progressive rod-cone degeneration in miniature poodles. *Invest Ophthalmol Vis Sci* **23,** 610–630
15. Aguirre, G., and O'Brien, P. (1986) Morphological and biochemical studies of canine progressive rod-cone degeneration: ^{3}H-fucose autoradiography. *Invest. Ophthalmol. Vis. Sci.* **27,** 635–655
16. Skiba, N. P., Spencer, W. J., Salinas, R. Y., Lieu, E. C., Thompson, J. W., and Arshavsky, V. Y. (2013) Proteomic identification of unique photoreceptor disc components reveals the presence of PRCD, a protein linked to retinal degeneration. *J. Proteome Res.* **12,** 3010–3018
17. Kang, R., Wan, J., Arstikaitis, P., Takahashi, H., Huang, K., Bailey, A. O., Thompson, J. X., Roth, A. F., Drisdel, R. C., Mastro, R., Green, W. N., Yates, J. R., 3rd, Davis, N. G., and El-Husseini, A. (2008) Neural palmitoyl-proteomics reveals dynamic synaptic palmitoylation. *Nature* **456,** 904–909
18. Linder, M. E., and Deschenes, R. J. (2007) Palmitoylation: policing protein stability and traffic. *Nat. Rev. Mol. Cell Biol.* **8,** 74–84
19. Yeste-Velasco, M., Linder, M. E., and Lu, Y. J. (2015) Protein *S*-palmitoylation and cancer. *Biochim. Biophys. Acta* **1856,** 107–120
20. Chamberlain, L. H., and Shipston, M. J. (2015) The physiology of protein *S*-acylation. *Physiol. Rev.* **95,** 341–376
21. Maeda, A., Okano, K., Park, P. S., Lem, J., Crouch, R. K., Maeda, T., and Palczewski, K. (2010) Palmitoylation stabilizes unliganded rod opsin. *Proc. Natl. Acad. Sci. U.S.A.* **107,** 8428–8433
22. Wang, Z., Wen, X. H., Ablonczy, Z., Crouch, R. K., Makino, C. L., and Lem, J. (2005) Enhanced shutoff of phototransduction in transgenic mice expressing palmitoylation-deficient rhodopsin. *J. Biol. Chem.* **280,** 24293–24300
23. Forrester, M. T., Hess, D. T., Thompson, J. W., Hultman, R., Moseley, M. A., Stamler, J. S., and Casey, P. J. (2011) Site-specific analysis of protein *S*-acylation by resin-assisted capture. *J. Lipid Res.* **52,** 393–398
24. Majumder, A., Pahlberg, J., Boyd, K. K., Kerov, V., Kolandaivelu, S., Ramamurthy, V., Sampath, A. P., and Artemyev, N. O. (2013) Transducin translocation contributes to rod survival and enhances synaptic transmission from rods to rod bipolar cells. *Proc. Natl. Acad. Sci. U.S.A.* **110,** 12468–12473
25. Linder, M. E., Middleton, P., Hepler, J. R., Taussig, R., Gilman, A. G., and Mumby, S. M. (1993) Lipid modifications of G proteins: α subunits are palmitoylated. *Proc. Natl. Acad. Sci. U.S.A.* **90,** 3675–3679
26. Ovchinnikov, Yu. A., Abdulaev, N. G., and Bogachuk, A. S. (1988) Two adjacent cysteine residues in the C-terminal cytoplasmic fragment of bovine rhodopsin are palmitylated. *FEBS Lett.* **230,** 1–5
27. Ramamurthy, V., Niemi, G. A., Reh, T. A., and Hurley, J. B. (2004) Leber congenital amaurosis linked to AIPL1: a mouse model reveals destabilization of cGMP phosphodiesterase. *Proc. Natl. Acad. Sci. U.S.A.* **101,** 13897–13902
28. Matsuda, T., and Cepko, C. L. (2007) Controlled expression of transgenes introduced by *in vivo* electroporation. *Proc. Natl. Acad. Sci. U.S.A.* **104,** 1027–1032
29. Gentilini, F., Rovesti, G. L., and Turba, M. E. (2009) Real-time detection of the mutation responsible for progressive rod-cone degeneration in Labrador Retriever dogs using locked nucleic acid TaqMan probes. *J. Vet. Diagn. Invest.* **21,** 689–692
30. Martin, B. R., and Cravatt, B. F. (2009) Large-scale profiling of protein palmitoylation in mammalian cells. *Nat. Methods* **6,** 135–138
31. Martin, B. R., Wang, C., Adibekian, A., Tully, S. E., and Cravatt, B. F. (2012) Global profiling of dynamic protein palmitoylation. *Nat. Methods* **9,** 84–89
32. Levy, A. D., Devignot, V., Fukata, Y., Fukata, M., Sobel, A., and Chauvin, S. (2011) Subcellular Golgi localization of stathmin family proteins is promoted by a specific set of DHHC palmitoyl transferases. *Mol. Biol. Cell* **22,** 1930–1942
33. Fernandes, A. F., Zhou, J., Zhang, X., Bian, Q., Sparrow, J., Taylor, A., Pereira, P., and Shang, F. (2008) Oxidative inactivation of the proteasome in retinal pigment epithelial cells: a potential link between oxidative stress and up-regulation of interleukin-8. *J. Biol. Chem.* **283,** 20745–20753
34. Kolandaivelu, S., Huang, J., Hurley, J. B., and Ramamurthy, V. (2009) AIPL1, a protein associated with childhood blindness, interacts with α-subunit of rod phosphodiesterase (PDE6) and is essential for its proper assembly. *J. Biol. Chem.* **284,** 30853–30861
35. Addison, J. B., Koontz, C., Fugett, J. H., Creighton, C. J., Chen, D., Farrugia, M. K., Padon, R. R., Voronkova, M. A., McLaughlin, S. L., Livengood, R. H., Lin, C. C., Ruppert, J. M., Pugacheva, E. N., and Ivanov, A. V. (2015) KAP1 promotes proliferation and metastatic progression of breast cancer cells. *Cancer Res.* **75,** 344–355
36. Beltran, W. A., Boye, S. L., Boye, S. E., Chiodo, V. A., Lewin, A. S., Hauswirth, W. W., and Aguirre, G. D. (2010) rAAV2/5 gene-targeting to rods: dose-dependent efficiency and complications associated with different promoters. *Gene Ther.* **17,** 1162–1174
37. Khani, S. C., Pawlyk, B. S., Bulgakov, O. V., Kasperek, E., Young, J. E., Adamian, M., Sun, X., Smith, A. J., Ali, R. R., and Li, T. (2007) AAV-mediated expression targeting of rod and cone photoreceptors with a human rhodopsin kinase promoter. *Invest. Ophthalmol. Vis. Sci.* **48,** 3954–3961
38. Greaves, J., and Chamberlain, L. H. (2007) Palmitoylation-dependent protein sorting. *J. Cell Biol.* **176,** 249–254
39. Siegert, S., Cabuy, E., Scherf, B. G., Kohler, H., Panda, S., Le, Y. Z., Fehling, H. J., Gaidatzis, D., Stadler, M. B., and Roska, B. (2012) Transcriptional code and disease map for adult retinal cell types. *Nat. Neurosci.* **15,** 487–495, S1–S2

40. Murphy, D., Singh, R., Kolandaivelu, S., Ramamurthy, V., and Stoilov, P. (2015) Alternative splicing shapes the phenotype of a mutation in *BBS8* to cause nonsyndromic retinitis pigmentosa. *Mol. Cell. Biol.* **35,** 1860–1870
41. Noritake, J., Fukata, Y., Iwanaga, T., Hosomi, N., Tsutsumi, R., Matsuda, N., Tani, H., Iwanari, H., Mochizuki, Y., Kodama, T., Matsuura, Y., Bredt, D. S., Hamakubo, T., and Fukata, M. (2009) Mobile DHHC palmitoylating enzyme mediates activity-sensitive synaptic targeting of PSD-95. *J. Cell Biol.* **186,** 147–160
42. Fukata, Y., and Fukata, M. (2010) Protein palmitoylation in neuronal development and synaptic plasticity. *Nat. Rev. Neurosci.* **11,** 161–175
43. Gelabert-Baldrich, M., Soriano-Castell, D., Calvo, M., Lu, A., Viña-Vilaseca, A., Rentero, C., Pol, A., Grinstein, S., Enrich, C., and Tebar, F. (2014) Dynamics of KRas on endosomes: involvement of acidic phospholipids in its association. *FASEB J.* **28,** 3023–3037
44. Williams, C. L. (2003) The polybasic region of Ras and Rho family small GTPases: a regulator of protein interactions and membrane association and a site of nuclear localization signal sequences. *Cell. Signal.* **15,** 1071–1080
45. Salaun, C., Greaves, J., and Chamberlain, L. H. (2010) The intracellular dynamic of protein palmitoylation. *J. Cell Biol.* **191,** 1229–1238
46. Roberts, B. J., Johnson, K. E., McGuinn, K. P., Saowapa, J., Svoboda, R. A., Mahoney, M. G., Johnson, K. R., and Wahl, J. K., 3rd. (2014) Palmitoylation of plakophilin is required for desmosome assembly. *J. Cell Sci.* **127,** 3782–3793